

1 **Differential Expression of Gluconeogenesis-Related Transcripts in a Freshwater**  
2 **Zooplankton Model Organism Suggests a Role of the Cori Cycle in Hypoxia Tolerance**

3

4 M. C. Malek<sup>1,2</sup>, J.R. Behera<sup>1</sup>, A. Kilaru<sup>1</sup> and L. Y. Yampolsky<sup>1,3</sup>

5

6 <sup>1</sup>Department of Biological Sciences, East Tennessee State University, Johnson City TN 37614, USA

7 <sup>2</sup>Present address: Department of Cell and Developmental Biology, Vanderbilt University, Nashville, TN

8 37240, USA

9 <sup>3</sup>Corresponding author: [yampolsk@etsu.edu](mailto:yampolsk@etsu.edu)

10

11

12

13

14

15

16

17

18

19

20

21

22

23

24

25

26

27

28

29 **Abstract**

30 1. Gluconeogenesis (GNG) is the process of regenerating glucose and NAD<sup>+</sup> that allows continuing ATP  
31 synthesis by glycolysis during fasting or in hypoxia. Recent data from *C. elegans* and crustaceans  
32 challenged with hypoxia show differential and tissue-specific expression of GNG-specific genes.

33 2. Here we report differential expression of several GNG-specific genes in the head and body of a model  
34 organism, *Daphnia magna*, a planktonic crustacean, in normoxic and acute hypoxic conditions. We predict  
35 that GNG-specific transcripts will be enriched in the body, where most of the fat tissue is located, rather  
36 than in the head, where the tissues critical for survival in hypoxia, the central nervous system and  
37 locomotory muscles, are located. We measured the relative expression of GNG-specific transcripts in each  
38 body part by qRT-PCR and normalized them by either the expression of a reference gene or the rate-  
39 limiting glycolysis enzyme pyruvate kinase (PK).

40 3. Our data show that of the three GNG-specific transcripts tested, pyruvate carboxylase (PC) showed no  
41 differential expression in either the head or body. Phosphoenolpyruvate carboxykinase (PEPCK-C), on the  
42 other hand, is upregulated in hypoxia in both body parts. Fructose-1,6-bisphosphatase (FBP) is upregulated  
43 in the body relative to the head and upregulated in hypoxia relative to normoxia, with a stronger body effect  
44 in hypoxia when normalized by PK expression.

45 4. These results support our hypothesis that *Daphnia* can survive hypoxic conditions by implementing the  
46 Cori cycle, where body tissues supply glucose and NAD<sup>+</sup> to the brain and muscles, enabling them to  
47 continuously generate ATP by glycolysis.

48

49

50

51

52 Keywords: gluconeogenesis, glycolysis, hypoxia, *Daphnia*, differential gene expression, Cori cycle

## 54 **Introduction**

55 The role of the Cori cycle or gluconeogenesis (GNG) has been well characterized in humans and other  
56 mammals, where products of glycolysis are utilized in the liver to resupply muscles and other critical tissues  
57 with glucose and NAD<sup>+</sup>, thus allowing glycolysis to continuously generate ATP during bursts of muscular  
58 activity or while in hypoxic or fasting conditions [1-6]. In some other vertebrates adapted to either periodic  
59 fasting[7] or hypoxia[8], the Cori cycle emerges as a key element of adaptation to environmental extremes.  
60 The GNG pathway utilizes lactate generated through the anaerobic catabolism of pyruvate as a precursor for  
61 glucose synthesis. This multi-step process is assisted by the respective glycolytic enzymes catalyzing the  
62 reverse reactions, except for the exclusive involvement of phosphoenolpyruvate carboxykinase (cytosolic  
63 PEPCK-C and mitochondrial PEPCK-M), fructose 1,6-bisphosphatase (FBP), and glucose 6-phosphatase in  
64 GNG[6] (Fig. 1). The upregulation of GNG-specific genes, primarily PEPCK paralogs, in hypoxia and the  
65 role of hypoxia-inducible factor (HIF-1) in this upregulation have been reliably demonstrated in mammalian  
66 models[9-11].

67 However, little data is available on GNG and the Cori cycle in aquatic invertebrates like  
68 crustaceans. Aquatic organisms are more likely to experience periods of hypoxia than terrestrial ones, as  
69 oxygen solubility and diffusion rates in water are low, and its availability is highly dependent on  
70 temperature, the respiratory activity of aerobic heterotrophs, and the non-biological oxidation of organic  
71 matter. Therefore, it is important to examine GNG as a possible mechanism of hypoxic survival to  
72 understand the ability of organisms to cope with episodes of high temperatures and low oxygen availability  
73 in their natural habitats.

74 Studies on the decapod shrimp *Litopenaeus vannamei* indicate tissue-specific expression of GNG-  
75 related genes are consistent with the role of GNG in providing glucose to fuel muscles during hypoxia. The  
76 hepatopancreas in crustaceans, an organ that is functionally analogous to the vertebrate liver, shows higher  
77 expression of *pyruvate carboxylase (PC)* [12], PEPCK-C and PEPCK-M [13], and FBP [14,15] relative to  
78 muscle or gill tissues. Importantly, this tissue-specific gene expression is further enhanced by hypoxia  
79 [12,13,15]. Furthermore, glucose-6-phosphatase, one of the rate-limiting enzymes of glycolysis, shows a  
80 reverse response pattern to hypoxia, where it is upregulated in the gills but not in the hepatopancreas [16].  
81 These results are consistent with the operation of the Cori cycle to allow hypoxia tolerance, with the  
82 hepatopancreas completing the GNG phase of the cycle and supplying tissues like muscles with glucose and  
83 NAD<sup>+</sup>. We expect this mechanism is likely conserved across invertebrates, as a similar differential  
84 expression was observed in the nematode *Caenorhabditis elegans* [17].

85 We have previously analyzed differential gene expression in response to mild chronic and severe  
86 acute hypoxia in a classic model organism for aquatic ecophysiology, *Daphnia magna* [18] revealing that  
87 while only a small subset of abundant transcripts showed differential expression responses under mild

88 chronic hypoxic conditions, many, including the GNG-specific PEPCK-C, showed upregulation in acute  
89 severe hypoxia. Aralar1, a mitochondrial carrier protein that transports aspartate from the mitochondria to  
90 the cytosol, also showed upregulation in hypoxia. The function of Aralar1 is critical for GNG, as it allows  
91 bypassing pyruvate as the starting point of the pathway by converting aspartate to oxaloacetate, a PEPCK-C  
92 substrate that converts to phosphoenolpyruvate in the cytosol.

93  
94 The goal of this study was to examine the differential expression of GNG-related enzymes PC,  
95 PEPCK-C, and FBP and the Aralar1 transporter separately in the head and body of hypoxia-challenged vs.  
96 normoxic control *Daphnia*. For *Daphnia* to survive in an acute hypoxic state, metabolic processes must be  
97 altered to allow alternative sources of glucose through GNG. We hypothesize that if GNG is upregulated as  
98 part of the Cori cycle, the relative abundance of transcripts should correspond to either the head or the body,  
99 with the body containing the majority of GNG transcripts while the head undergoes glycolysis steps (Figure  
100 1). To that end, we used both a reference gene unrelated to glucose metabolism and a rate-limiting  
101 glycolysis enzyme, pyruvate kinase, as normalization controls to infer the relative expression of GNG-  
102 related transcripts, thus emphasizing the relative expression of the two opposing Cori cycle pathways in the  
103 heads and bodies of *Daphnia*.

104

## 105 **Materials and methods**

### 106 ***Daphnia* clones and culture**

107 *Daphnia magna* stocks used in this study were obtained from the Basel University *Daphnia* Stock  
108 Collection (Basel, Switzerland) and maintained locally since 2016. The IDs of the four stocks used were FI-  
109 FSP1-16-2, GB-EL75-69, HU-K-6, and IL-M1-8; details of the provenance of these *D. magna* clones are  
110 supplied on Table 1 in Ekwudo et al. 2022. Hereafter, we refer to these clones by the first two letters of  
111 their Basel stock IDs. Previous longevity studies indicate that these clones differ significantly in their  
112 lifespan and acute hypoxia tolerance, with FI and IL being the short-lived, hypoxia-tolerant clones, and GB  
113 and HU showing higher longevity but lower hypoxia tolerance [18]. Stocks were maintained in modified  
114 ADaM zooplankton medium (Ref. [19]; <https://evolution.unibas.ch/ebert/lab/adam.htm>) at the density of  
115 one adult *Daphnia* per 20 mL, at 20 °C under 16h:8h L:D photoperiod and fed green alga *Scenedesmus*  
116 *acutus* Meyen (current nomenclature *Tetradesmus obliquus* (Turpin) M. J. Wynne) at the concentration of  
117 10<sup>5</sup> cells per mL per day. Newborn individuals of each of the four clones were collected within 24 h of birth  
118 and placed in groups of 10 in 100 mL jars, with the density reduced to one *Daphnia* per 20 mL at maturity  
119 (day 6-8), and maintained with food added daily, water changed, and neonates removed twice weekly. The  
120 four clones used were characterized by their lactate:pyruvate ratio in normoxic and acute hypoxic  
121 conditions, as described below.

122  
123  
124  
125  
126  
127  
128  
129  
130  
131  
132  
133  
134  
135  
136  
137  
138  
139  
140  
141  
142  
143  
144

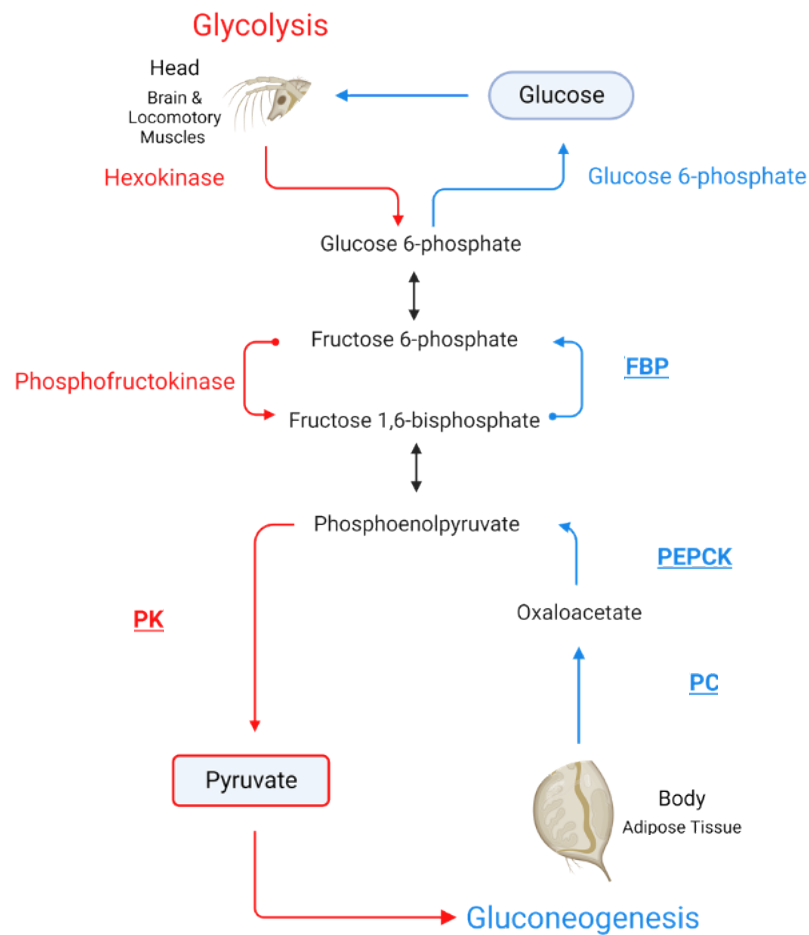


Fig. 1. Schematic representation of the Cori cycle. Only those steps of glycolysis (red) and gluconeogenesis (blue) that are accomplished by different enzymes are labeled. The enzymes labeled are rate-limiting for each of the two branches of the cycle. Enzymes analyzed in this study are shown in bold, underlined type. FBP: fructose-1,6-bisphosphatase; PC: pyruvate carboxylase; PEPCK: phosphoenolpyruvate carboxykinase; PK: pyruvate kinase.

145  
146  
147  
148  
149  
150  
151

152 ***Acute hypoxia exposure and lactate:pyruvate ratio measurements***

153 *Daphnia* females maintained as described above until the age of 15-25 days were randomly assigned to  
154 control and hypoxia treatments. Hypoxia treatment individuals were placed individually in 10-mL screw-  
155 cap vials filled with 20 °C ADaM water deoxygenized to <1 mg O<sub>2</sub>/L by intense bubbling with nitrogen.  
156 Oxygen concentration was maintained by an Extech DO210 dissolved oxygen meter. Simultaneously, the  
157 control *Daphnia* were transferred into fresh vials containing fully oxygenized (>8 mg O<sub>2</sub>/L) ADaM. No  
158 food was added to either the hypoxia or control vials. *Daphnia* were harvested after 12 hours of exposure.  
159 Typically, no mortality occurs in 12 hours at 1 mg O<sub>2</sub>/L, with survival times ranging between 17 and 30  
160 hours[18]. This experiment was conducted in two randomized blocks on two different dates, with 48 and 16  
161 *Daphnia* used in each block.

162

163 Whole *Daphnia* females from either control or acute hypoxia treatments were homogenized in 100  
164 µL of RO water using a bead beater with 0.15 mm ZrO beads and centrifuged for 4 min at 4 °C. The  
165 supernatant was then used to determine lactate and pyruvate concentrations using CellBioLabs®  
166 colorimetric kits (Cat. #s MET-5012 and MET-5125, respectively), according to the manufacturer's  
167 protocol, scaled down to 50 µL reactions, each containing 20 µL of supernatant. Absorbance was measured  
168 in 384-well plates on a BioTek Synergy plate reader at room temperature at 490 and 570 nm for lactate and  
169 pyruvate, respectively. In parallel, soluble protein content in the supernatant was measured by the Bradford  
170 method to normalize lactate and pyruvate concentrations per mg of protein.

171 Based on the results, we then selected the hypoxia-tolerant clone IL, characterized by the highest  
172 lactate:pyruvate ratio in hypoxia, for further qRT-PCR analyses.

173

174 ***Differential gene expression quantification***

175 Total RNA was extracted using the RNeasy Mini Kit (Qiagen) from the heads and bodies of 15 days old *D.*  
176 *magna* females (clone IL) exposed to acute hypoxia treatment or normoxia as described above. 10 females  
177 per sample were used for the RNA extraction, and four such samples were prepared for each condition. The  
178 RNA concentration was measured by Nanodrop, and samples were diluted to a final concentration of 20  
179 ng/µL in RNase-free water. qRT-PCR was done using the qScript One-Step SYBR Green qRT-PCR Kit  
180 (Quantabio) according to the manufacturer's protocol, using gene-specific primers (Table 1). A total of 80  
181 ng of RNA was used as input in a 20 µL reaction mixture, and all the reactions were carried out using an  
182 Illumina Eco Real-time PCR system. Four biological replicate samples in two technical replicates were  
183 used. The cDNA synthesis was performed at 50 °C for 10 minutes using the primers specific for the genes  
184 (Table 1), followed by polymerase activation at 95 °C for 10 minutes. PCR cycles were carried out at 95 °C  
185 for 10s, followed by 60 °C for 20s, for 40 cycles. Fluorescence signals (Channel 1; for SYBR Green) were

186 detected after each cycle. The reference genes were chosen following Ref[20]. We tested *D. magna*  
187 orthologs of the following proposed internal reference genes for constant expression: X-box binding protein  
188 1 (*Xbp1*), TATA-box binding protein (*Tbp*), and syntaxin-16 (*Stx16*). Among these, *Xbp1* showed no  
189 difference in expression between the control and hypoxia treatments and was thus chosen as the reference  
190 gene. The quantification cycle (Cq) values for each gene expression were determined from the amplification  
191 curves at a threshold value set at 0.02, and the relative expression of GNG-related genes was expressed as -  
192  $\Delta Cq$  (Rao et al. 2013). For further comparison relative to the pace of glycolysis, corresponding gene  
193 expressions were also normalized against that of the muscular isoform pyruvate kinase (PK) gene that  
194 catalyzes one of the rate-limiting steps of glycolysis.

195 Table 1. qRT-PCR primers used for GNG-related and reference genes. Xbp1, X-box binding protein 1; Tbp,  
 196 TATA-box binding protein; Stx16, syntaxin-16; Arlar1; FBP, fructose 1,6-bisphosphotase; PEPCK-C,  
 197 cytoplasmic phosphoenolpyruvate carboxykinase; PC, mitochondrial pyruvate carboxylase; PK, pyruvate  
 198 kinase, muscle isoform.

199

200 Table 1: Gene-specific primers used in qRT-PCR.

201

Gene	Accession	Primer	5'-3' Primer sequence	Product size, bp
Xbp1	XM_032923654	Forward	CAGAGGCTTGATCACATGAC	150
		Reverse	GTGATTGTTCTCTGCCCTAAG	
Tbp	XM_032935699	Forward	CTGACTCACAGCCAGTTTAG	130
		Reverse	GAAC TTTGGCGCCAGTAA	
Stx16	XM_032933438	Forward	ACCTGAACAAGATAAAGTCACG	124
		Reverse	TGGCTCATAACCCTTGGA	
Aralar1	XM_032929071	Forward	TCCTTTGTTGGCGAGTTAAT	156
		Reverse	GACCAGATCGTTAGTTGTGAG	
FBP	XM_032922068	Forward	CAAAGAAAGAGGGTGCGAAG	106
		Reverse	TGTGGCAGGGTCATGAATA	
PEPCK-C	XM_045175641	Forward	TCATCCAATGCCAGAGA	108
		Reverse	CTATTACCGAGCCAATCCTTAG	
PC	XM_032936339	Forward	GCCAAGGTCATCACAGAAA	150
		Reverse	CACCTGCTCATTCGTTATCC	
PK	XM_045169465	Forward	AGCGGAGAAACAGCAAAG	129
		Reverse	AGTAACGACCATGCCAGA	

202

203

#### 204 **Data analysis**

205 Lactate and pyruvate content and qRT-PCR data were analyzed using Residual Maximum  
 206 Likelihood (REML) ANOVA using JMP (Ver. 16, SAS Institute 2016), with protein-normalized lactate and  
 207 pyruvate concentrations and their ratio, or relative expression, respectively, as the response variables. The  
 208 main effects in the model were clones and acute hypoxia exposure. The date of measurement was included  
 209 in the model as a random block effect. For qRT-PCR data, the biological replicate was included in the  
 210 analysis as a random block effect. Table-wide sequential Bonferroni-adjusted P-values[20] were calculated  
 211 for each table of results.

212 **Results**

213 ***Lactate and pyruvate content***

214 Here we examined the differences in protein-normalized concentrations of lactate and pyruvate and their  
 215 ratio under hypoxic and normoxic conditions among four *D. magna* clones (Table 2, Fig 2). Lactate  
 216 concentration significantly increased in hypoxia but did not differ among the clones, while pyruvate  
 217 concentration did not increase in hypoxia but showed a strong clone effect, with the IL clone demonstrating  
 218 the lowest levels of pyruvate. As the results indicate, the lactate:pyruvate ratio showed both clone and  
 219 hypoxia effects, with the increased lactate:pyruvate ratio after exposure to acute hypoxia being largely due  
 220 to the increase in lactate concentration, whereas interclonal differences were largely due to differences in  
 221 pyruvate concentration. There were no interaction effects between clones and hypoxia in either lactate or  
 222 pyruvate concentrations or their ratio (Table 2).

223  
 224 Table 2. Residual maximum likelihood (REML) analysis of variance of the differences in protein-  
 225 normalized concentrations of lactate and pyruvate and their ratio among clones and between hypoxia  
 226 treatment and normoxic control. P<0.025 shown in italics; P<0.001 in bold. Sequential Bonferroni-  
 227 corrected P-values are shown to the right of individually significant P-values

228

Source	DF	DFDen	F Ratio	P	P <sub>adj</sub>
<b>Response Lac/Pyr</b>					
Clone	3	55	8.69	<b>&lt;0.0001</b>	<b>&lt;0.001</b>
Hypoxia	1	47.02	25.43	<b>&lt;0.0001</b>	<b>&lt;0.001</b>
Clone*Hypoxia	3	55	1.27	0.29	
<b>Response Lac, mM/mg Prot</b>					
Clone	3	55	0.46	0.71	
Hypoxia	1	55.9	63.47	<b>&lt;0.0001</b>	<b>&lt;0.001</b>
Clone*Hypoxia	3	55	0.397	0.75	
<b>Response Pyr, mM/mg Prot</b>					
Clone	3	55	7.02	<b>0.0004</b>	<b>0.0024</b>
Hypoxia	1	55.89	6.18	<i>0.0159</i>	0.08
Clone*Hypoxia	3	55	0.08	0.97	

229

230  
231  
232  
233  
234  
235  
236  
237  
238  
239  
240  
241  
242  
243  
244  
245  
246  
247  
248  
249  
250  
251  
252  
253  
254  
255  
256  
257  
258  
259  
260  
261

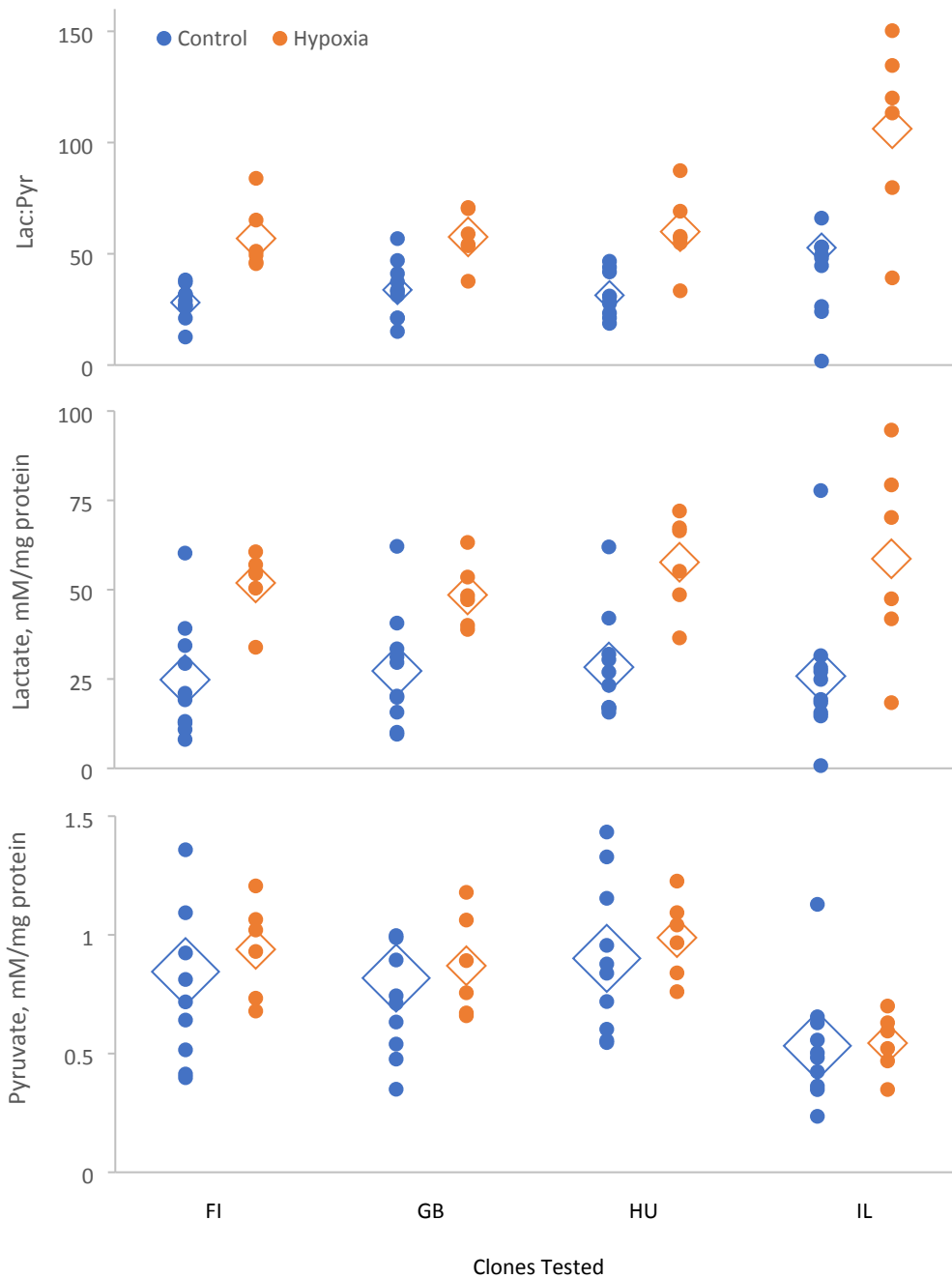


Fig. 2. Lactate:pyruvate ratio and protein-normalized lactate and pyruvate concentration in whole-body extracts in *Daphnia* from normoxic control (blue) and 12 h exposure to acute hypoxia (orange). Diamonds represent means; a diamond's height represents the SE of the mean.

262 ***Differential gene expression***

263 The results of differential expression analysis by qPCR were somewhat different depending on which  
264 transcript was used for normalization: a carbohydrate metabolism-independent housekeeping reference gene  
265 Xbp1 or the glycolysis rate-limiting PK (Fig. 1), even though PK itself showed no significant differences  
266 between either oxygen levels or body parts (Table 3, Fig. 3). Normalization of GNG-specific transcripts by  
267 Xbp1 reflects general levels of expression; normalization by PK reflects the relative activity of the GNG vs.  
268 glycolysis branches of the Cori cycle. Of the four GNG-related transcripts tested, the transport protein  
269 Aralar1 transcript, contrary to predictions, showed a slight downregulation in hypoxia. PC showed no  
270 evidence of differential expression regardless of which reference was used for normalization (Table 3). The  
271 other two transcripts, PEPCK-C and FBP, showed hypoxia-related differential expression. Both PEPCK-C  
272 and FBP were upregulated in hypoxia when normalized by Xbp1 (tentatively significant after multiple test  
273 correction); FBP was both upregulated in hypoxia and in the bodies, relative to the heads, as predicted, with  
274 the hypoxia upregulation being stronger in the head than in the body (Table 3; Fig. 3).

275

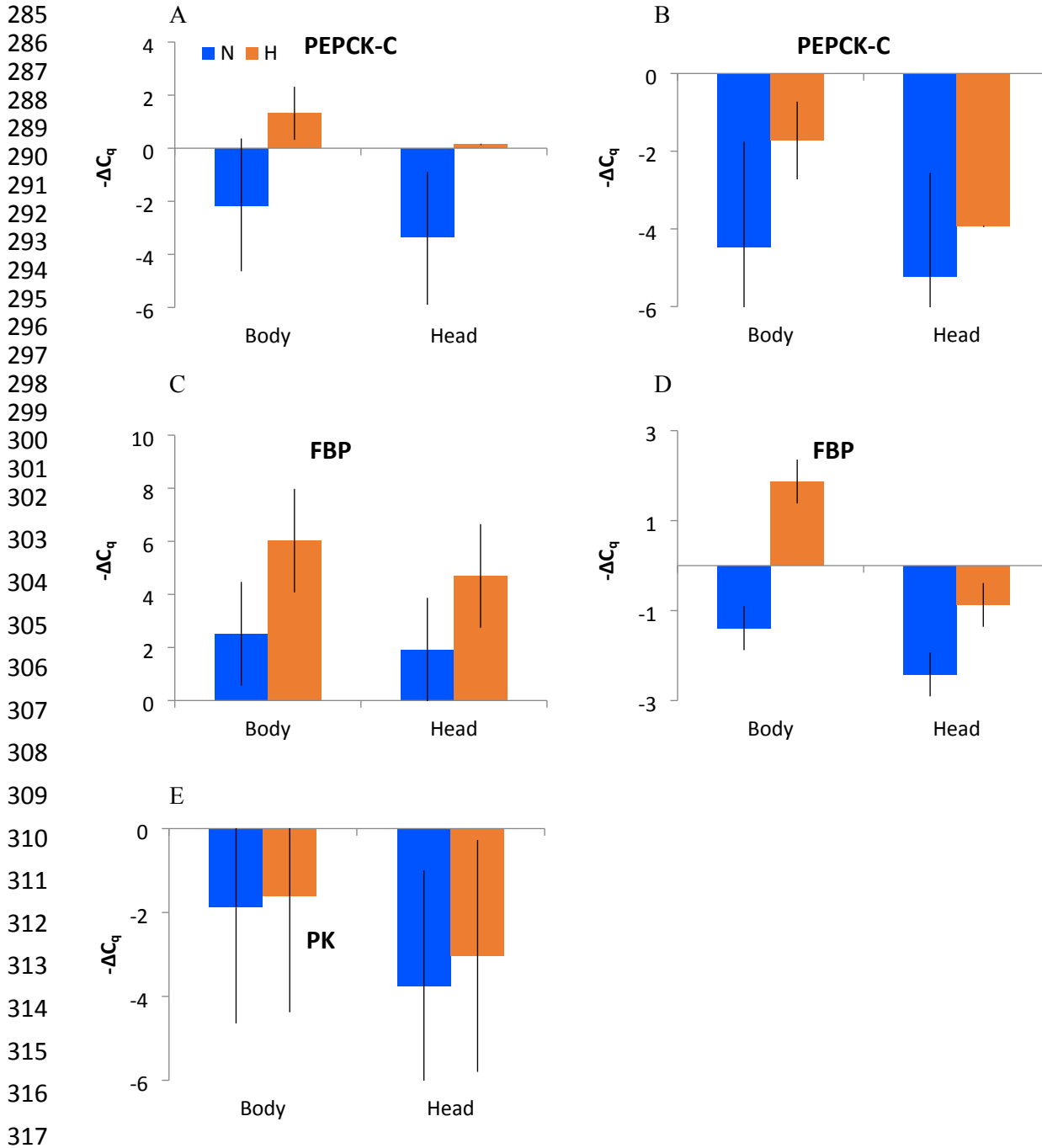
276

277 Table 3. Residual maximum likelihood (REML) analysis of variance of the effects of hypoxia (normoxic  
 278 control vs. 12 hours at <1 mg/L O<sub>2</sub>) and body part (head vs. body) on transcript abundance (-ΔCq) for four  
 279 GNG-related transcripts normalized either by the general housekeeping reference gene encoding X-box  
 280 binding protein (Xbp1) or glycolysis-specific pyruvate kinase (PK). P<0.025 shown in italics; P<0.001 in  
 281 bold. Sequential Bonferroni-adjusted P-values shown on the right on individually significant P-values.  
 282

Transcript	Source	Normalized by Xbp1					Normalized by PK				
		DF	DF <sub>Den</sub>	F	P	P <sub>adj</sub>	DF	DF <sub>Den</sub>	F	P	P <sub>adj</sub>
Aralar1	Hypoxia	1	7.94	7.90	<i>0.023</i>	0.12	1	8.09	1.85	0.21	
	BodyPart	1	7.94	0.08	0.78		1	8.29	0.19	0.67	
	Hypoxia* BodyPart	1	7.94	0.21	0.66		1	8.09	0.001	0.99	
PC	Hypoxia	1	11.1	1.11	0.32		1	11.8	1.48	0.25	
	BodyPart	1	11.1	0.91	0.36		1	11.8	0.17	0.69	
	Hypoxia* BodyPart	1	11.1	0.40	0.54		1	11.8	0.39	0.54	
PEPCK-C	Hypoxia	1	13.1	7.43	<i>0.017</i>	0.10	1	13	4.23	0.06	
	BodyPart	1	13.1	0.83	0.38		1	13	2.28	0.16	
	Hypoxia* BodyPart	1	13.1	0	1		1	13	0.50	0.49	
FBP	Hypoxia	1	12	9.11	<i>0.011</i>	0.08	1	12	46.21	<b>&lt;0.0001</b>	<b>&lt;0.001</b>
	BodyPart	1	12	0.86	0.37		1	12	28.44	<b>0.0002</b>	<b>0.0016</b>
	Hypoxia* BodyPart	1	12	0.12	0.73		1	12	5.871	0.032	0.13
PK	Hypoxia	1	15	0.13	0.72						
	BodyPart	1	15	1.48	0.24						
	Hypoxia* BodyPart	1	15	0.03	0.87						

283

284



318 Fig. 3. Relative expression ( $-\Delta C_q$ ) of PEPCK-C (A, B), FBP (C, D), and PK (E) transcripts normalized by  
319 Xbp (A, C, E) and PK (B, D). Error bars represent standard error. Higher values indicate higher expression;  
320  $-\Delta C_q$  difference of 1 corresponds to two-fold difference in transcript abundance. Colors as on Fig. 2.  
321

## 322 Discussion

323 The Cori cycle is an adaptation to intense bouts of muscular activity in larger animals, where it is difficult  
324 to supply sufficient oxygen for oxidative phosphorylation in muscles during peak ATP demand [5].  
325 However, this is a costly way of generating ATP, as for every mole of ATP generated by glycolysis in the  
326 muscles, three moles are spent in the GNG branch of Cori cycle, making it unsustainable in the long term.  
327 However, even small organisms may have to resort to GNG to regenerate glucose in hypoxic conditions.  
328 For example, zooplankton organisms like *Daphnia* must continuously swim (typically upward) to avoid  
329 hypoxic layers or spots within a lake or pond, and this is likely a subject for selection.

330  
331 In *Daphnia* and other cladocerans, the head contains major locomotory muscles, namely the ones  
332 driving the 2<sup>nd</sup> (swimming) antenna, in addition to the mitochondria-rich ATP-consuming central neural  
333 system (Ref. [21], Fig. 1.3). Thus, the head tissues and organs are likely to be the primary consumers of  
334 glucose synthesized by GNG in conditions when glycolysis is the main source of ATP. While the “classic”  
335 mammalian GNG-active organs, the liver and kidneys, do not have direct counterparts in *Daphnia* anatomy,  
336 we hypothesize that the adipose tissue, located in the thorax and the abdomen, may be the main site of  
337 GNG. Lactate and pyruvate metabolism, including the starting points of gluconeogenesis such as the  
338 conversion of pyruvate to oxaloacetate by PC, is known to be active in adipose tissue in both mammals and  
339 arthropods [22]. Therefore, we hypothesize that the “body” (thorax and abdomen) may be the donor of  
340 glucose produced by GNG in the Cori cycle operating in *Daphnia* under hypoxic conditions, suggesting  
341 differential expression of the GNG and glycolysis-related genes in the body and the head. And a further  
342 prediction made was that acute hypoxia should augment this differentiation.

343  
344 These predictions were tested in a qRT-PCR experiment, measuring GNG-related transcript  
345 abundance separately in the heads and bodies of individuals from the IL *Daphnia* clone. We selected this  
346 clone from a panel of four as it was the one characterized by the lowest pyruvate accumulation in tissues,  
347 hypothetically indicating the utilization of pyruvate for lactic fermentation and/or GNG. This clone has  
348 previously been demonstrated to be the most hypoxia-tolerant of the four clones tested [18]. We observed a  
349 significant upregulation of PEPCK-C and FBP (but not of PC) in hypoxia in both body parts when  
350 normalized by a reference gene unrelated to carbohydrate metabolism (Fig. 3). We also observed a  
351 significant upregulation of FBP, a rate-limiting GNG enzyme, in hypoxia and in the body relative to the  
352 head, when normalized by PK, one of the rate-limiting enzymes of glycolysis. We therefore conclude that  
353 body/head compartmentalization of the glycolysis and GNG pathways is likely necessary for survival in  
354 hypoxia. Furthermore, we predicted the hypoxia-by-body part interaction with the hypoxia effect being

355 stronger in the body than in the head (Fig. 3); however, this predicted interaction effect was only marginally  
356 significant and did not survive multiple test correction.

357 It is yet to be tested if the same observation would be made with a less hypoxia-tolerant clone of *D.*  
358 *magna* (or in less hypoxia-tolerant species of zooplankton). Further studies would test if that variation in  
359 hypoxia tolerance, within and among zooplankton species, is maintained by the trade-offs between the  
360 ability to operate the Cori cycle in hypoxia and the GNG-associated costs of doing so when oxygen is  
361 abundant.

362

363

## 364 **Conclusions**

365 We observe upregulation of the genes encoding rate-limiting gluconeogenesis enzymes,  
366 cytoplasmic phosphoenolpyruvate carboxykinase (PEPCK-C) and fructose-1,6-bisphosphatase (FBP), in  
367 hypoxia within a hypoxia-tolerant clone of *Daphnia*. When normalized by the rate-limiting glycolysis  
368 enzyme pyruvate kinase, the upregulation of FBP is more pronounced in the body than in the head of  
369 *Daphnia*, indicating the potential role of the Cori cycle in sustaining glycolysis in the central nervous  
370 system and locomotory muscles during hypoxia.

371

## 372 **References**

373

- 374 1. Cori, C.F., & Cori, G.T. 1929. Glycogen formation in the liver from d- and l-lactic acid. *J Biol Chem*, 81,  
375 389–403.
- 376 2. Reichard, G. A., Jr., Moury N. F., Jr., Hochella, N. J., Patterson, A. L., & Weinhouse, S. 1963.  
377 Quantitative estimation of the Cori cycle in the human. *J. Biol. Chem*, 238, 495.
- 378 3. Cahill, G. F. 1970. Starvation in Man. *New England Journal of Medicine*, 282(12), 668–675.  
379 doi:10.1056/nejm197003192821209
- 380 4. Freminet, A., Poyart, C., Leclerc, L., & Gentil, M. 1976. Effect of fasting on the Cori cycle in rats. *FEBS*  
381 *Lett*, 66, 2, 328-331. doi: 10.1016/0014-5793(76)80532-7.PMID: 955096.
- 382 5. Cori, C.F. 1981. The glucose-lactic acid cycle and gluconeogenesis. *Current Topics in Cellular*  
383 *Regulation*, 18, 377-387.
- 384 6. Nelson, D.L., & Cox, M.M. 2005. *Lehninger Principles of Biochemistry* (Fourth ed.). New York: W.H.  
385 Freeman and Company. p. 543.
- 386 7. Champagne, C.D., Houser, D.S., & Crocker, D.E. 2005. Glucose production and substrate cycle activity  
387 in a fasting adapted animal, the northern elephant seal. *J Exp Biol.*, 208(Pt 5), 859-868. doi:  
388 10.1242/jeb.01476. PMID: 15755884.

- 389 8. Gupta, A., Varma, A., & Storey, K.B. 2021. New insights to regulation of fructose-1,6-bisphosphatase  
390 during anoxia in red-eared slider, *Trachemys scripta elegans*. *Biomolecules*, 11, 10, 1548. doi:  
391 10.3390/biom11101548. PMID: 34680181.
- 392 9. Choi, J.H., Park, M.J., Kim, K.W., Choi, Y.H., Park, S.H., An, W.G., Yang, U.S., & Cheong J. 2005.  
393 Molecular mechanism of hypoxia-mediated hepatic gluconeogenesis by transcriptional  
394 regulation. *FEBS Lett.*, 579(13), 2795-2801. doi: 10.1016/j.febslet.2005.03.097. PMID:  
395 15907483.
- 396 10. Hara, Y., & Watanabe, N. 2020. Changes in expression of genes related to glucose metabolism in liver  
397 and skeletal muscle of rats exposed to acute hypoxia. *Heliyon*, 6, 7, e04334. doi:  
398 10.1016/j.heliyon.2020.e04334. PMID: 32642586.
- 399 11. Owczarek, A., Gieczewska, K., Jarzyna, R., Jagielski, A.K., Kiersztan, A., Gruza, A., & Winiarska, K.  
400 2020. Hypoxia increases the rate of renal gluconeogenesis via hypoxia-inducible factor-1-  
401 dependent activation of phosphoenolpyruvate carboxykinase expression. *Biochimie*, 171-172, 31-  
402 37. doi: 10.1016/j.biochi.2020.02.002. PMID: 32045650.
- 403 12. Granillo-Luna, O.N., Hernandez-Aguirre, L.E., Peregrino-Uriarte, A.B., Duarte-Gutierrez, J., Contreras-  
404 Vergara, C.A., Gollas-Galvan, T., & Yepiz-Plascencia, G. 2022. The anaplerotic pyruvate  
405 carboxylase from white shrimp *Litopenaeus vannamei*: Gene structure, molecular  
406 characterization, protein modelling and expression during hypoxia. *Comp Biochem Physiol A*  
407 *Mol Integr Physiol*, 269, 111212. doi: 10.1016/j.cbpa.2022.111212. PMID: 35417748.
- 408 13. Reyes-Ramos CA, Peregrino-Uriarte AB, Cota-Ruiz K, Valenzuela-Soto EM, Leyva-Carrillo L, Yepiz-  
409 Plascencia G. 2018. Phosphoenolpyruvate carboxykinase cytosolic and mitochondrial isoforms  
410 are expressed and active during hypoxia in the white shrimp *Litopenaeus vannamei*. *Comp*  
411 *Biochem Physiol B Biochem Mol Biol*. 226:1-9. doi: 10.1016/j.cbpb.2018.08.001. PMID:  
412 30107223.
- 413 14. Cota-Ruiz, K., Peregrino-Uriarte, A.B., Felix-Portillo, M., Martínez-Quintana, J.A., & Yepiz-  
414 Plascencia, G. 2015. Expression of fructose 1,6-bisphosphatase and phosphofructokinase is  
415 induced in hepatopancreas of the white shrimp *Litopenaeus vannamei* by hypoxia. *Mar Environ*  
416 *Res*, 106, 1-9. doi: 10.1016/j.marenvres.2015.02.003. PMID: 25725474.
- 417 15. Cota-Ruiz, K., Leyva-Carrillo, L., Peregrino-Uriarte, A.B., Valenzuela-Soto, E.M., Gollas-Galván, T.,  
418 Gómez-Jiménez, S., Hernández, J., & Yepiz-Plascencia, G. 2016. Role of HIF-1 on  
419 phosphofructokinase and fructose 1,6-bisphosphatase expression during hypoxia in the white  
420 shrimp i. *Comp Biochem Physiol A Mol Integr Physiol*, 198,1-7. doi:  
421 10.1016/j.cbpa.2016.03.015. PMID: 27032338.

- 422 16. Hernández-Aguirre, L.E., Cota-Ruiz, K., Peregrino-Uriarte, A.B., Gómez-Jiménez, S., & Yepiz-  
423 Plascencia, G. 2021. The gluconeogenic glucose-6-phosphatase gene is expressed during oxygen-  
424 limited conditions in the white shrimp *Penaeus (Litopenaeus) vannamei*: Molecular cloning,  
425 membrane protein modeling and transcript modulation in gills and hepatopancreas. *J Bioenerg*  
426 *Biomembr*, 53, 4, 449-461. doi: 10.1007/s10863-021-09903-6. PMID: 34043143.
- 427 17. Vora, M., Pyontek, S.M., Popovitchenko, T., Matlack, T.L., Prashar, A., Kane, N.S., Favate, J., Shah,  
428 P., & Rongo, C. 2022. The hypoxia response pathway promotes PEP carboxykinase and  
429 gluconeogenesis in *C. elegans*. *Nature Communications*, 13, 1, 6168. doi: 10.1038/s41467-022-  
430 33849-x. PMID: 36257965.
- 431 18. Ekwudo MN, Malek MC, Anderson CE, Yampolsky LY. 2022. The interplay between prior selection,  
432 mild intermittent exposure, and acute severe exposure in phenotypic and transcriptional response  
433 to hypoxia. *Ecol Evol*. 12(10):e9319. doi: 10.1002/ece3.9319. PMID: 36248677.
- 434 19. Klüttgen B, U Dülmer, M Engels, H.T Ratte. 1994. ADaM, an artificial freshwater for the culture of  
435 zooplankton. *Water Research* 28 (3), 743-746. [https://doi.org/10.1016/0043-1354\(94\)90157-0](https://doi.org/10.1016/0043-1354(94)90157-0).
- 436 20. Holm, S. 1979. A simple sequentially rejective multiple test procedure. *Scandinavian Journal of*  
437 *Statistics*. 6 (2): 65–70.
- 438 20. Spanier, K.I., Leese, F., Mayer, C., Colbourne, J.K., Gilbert, D., Pfrender, M.E., & Tollrian, R. 2010.  
439 Predator-induced defenses in *Daphnia pulex*: selection and evaluation of internal reference genes  
440 for gene expression studies with real-time PCR. *BMC Mol Biol*, 11, 50. doi: 10.1186/1471-2199-  
441 11-50. PMID: 20587017.
- 442 21. Rao X., Huang. X., Zhou, Z., & Lin, X. 2013. An improvement of the  $2^{-(\Delta\Delta CT)}$  method for  
443 quantitative real-time polymerase chain reaction data analysis. *Biostat Bioinforma Biomath*, 3, 3,  
444 71-85. PMID: 25558171.
- 445 22. Smirnov, N.N. 2017) *Physiology of the Cladocera*. 2nd edition Academic Press.
- 446 23. Krycer, J.R., Quek, L.E., Francis, D., Fazakerley, D.J., Elkington, S.D., Diaz-Vegas, A., Cooke, K.C.,  
447 Weiss, F.C., Duan, X., Kurdyukov, S., Zhou, P.X., Tambar, U.K., Hirayama, A., Ikeda, S.,  
448 Kamei, Y., Soga, T., Cooney, G.J., & James, D.E. 2020. Lactate production is a prioritized  
449 feature of adipocyte metabolism. *J Biol Chem*, 295, 1, 83-98. doi: 10.1074/jbc.RA119.011178.  
450 PMID: PMC6952601.